How large is the ^{7}Be neutrino flux from the Sun?

L. Wolfenstein
Carnegie Mellon University, Pittsburgh, Pennsylvania 15213

P. I. Krastev
Institute for Advanced Study, Princeton, New Jersey 08540

(Received 18 October 1996)

On the basis of present solar neutrino observations and relaxing the constraints from solar models it is possible that most (or nearly all) of the flux of electron neutrinos detected comes from electron capture in ^{7}Be. These solutions arise from neutrino oscillations in which ν_e-ν_τ mixing suppresses high energy ν_e and ν_e-ν_μ mixing suppresses low energy ν_e as qualitatively suggested from some SO(10) grand unified models. The importance of future observations is emphasized. [S0556-2821(97)01007-2]

PACS number(s): 14.60.Pq, 12.15.Ff, 26.65.+t, 96.40.Tv

I. INTRODUCTION

Solar neutrinos provide the only direct evidence of the nuclear reactions that are believed to be the primary source of energy inside the Sun. Solar model calculations [1] show that the energy is produced mainly in the pp cycle which yields three major neutrino sources: (1) pp neutrinos with energies below 420 keV, (2) neutrinos from electron capture in ^{7}Be with a line spectrum and a main energy of 862 keV, and (3) the much rarer ^{8}B decay neutrinos with a spectrum up to 15 MeV. Three types of experiments have detected neutrinos: (1) the Kamiokande experiment [2] using neutrino-electron scattering sensitive only to ^{8}B neutrinos, (2) the Davis ^{37}Cl detector [3] sensitive primarily to ^{8}B but also to ^{7}Be neutrinos, and (3) the two gallium experiments GALLEX [4] and SAGE [5], sensitive to all three sources but, due to the rareness of ^{8}B neutrinos, primarily important for the pp and ^{7}Be sources. By combining the data from the three experiments one can try to determine the flux from each source that reaches the Earth.

In the standard analysis repeated in many papers [6] one uses the observed Kamiokande detection rate to determine the flux of ν_e from ^{8}B that reaches the Earth. One then applies the so-obtained constraint on the boron neutrino flux to the ^{37}Cl experiment and finds that the observed rate is explained by ^{8}B neutrinos allowing for few or no ^{7}Be neutrinos. If there are no ^{7}Be neutrinos, then one can understand the gallium results as being due primarily to pp neutrinos with flux equal to that of the standard solar model (SSM). Thus one concludes that there must exist neutrino oscillations that almost totally convert the ^{7}Be ν_e into another type of neutrino but have little effect on pp neutrinos. This leads to solutions for neutrino masses and mixing, in particular, the small angle Mikheyev-Smirnov-Wolfenstein (MSW) solution with $\Delta m^2 \approx 10^{-5}$ eV^2 and $\sin^2 2\theta \approx 10^{-2}$.

It is worth pointing out [7] that without oscillations one does not obtain a good fit to the data, even if all the solar neutrino fluxes are allowed to vary assuming arbitrary nonnegative values, subject only to the luminosity constraint. In this case the minimum $\chi^2_{\min} = 5.9$ and it occurs for zero CNO and beryllium neutrinos, boron neutrino flux equal to 0.35 of its standard solar model value of 6.62×10^6 cm^{-2} s^{-1}, and for a pp neutrino flux equal to that maximally allowed by the luminosity constraint value of 6.51×10^{10} cm^{-2} s^{-1}.

Recently a number of authors [8–11] have considered relaxing the constraints of the SSM in order to determine what is really known about the fluxes, at the same time allowing neutrino oscillations. One assumes only that the neutrinos arise from known nuclear reactions and that the presently observed luminosity is the result of these same reactions. The neutrino oscillation parameters Δm^2 and $\sin^2 2\theta$ are varied so as to fit present experiments with nonstandard solar neutrino fluxes. It turns out that solutions can be found even for neutrino fluxes vastly different from the ones in the SSM. An extreme possibility [12], which assumes the MSW solution as a solution, allows that nearly all of the solar energy arises from the CNO bicycle of nuclear reactions and nearly all of the ν_e observed in gallium and chlorine experiments are from ^{13}N and ^{15}O decays.

Here we consider the possibility that most or nearly all the ν_e observed are from ^{7}Be, the opposite of the ''conventional'' interpretation of solar neutrino experiments. While the radiochemical detectors measure directly the flux of ν_e from the Sun, neutrino-electron scattering detectors are also sensitive to ν_μ and ν_τ. Therefore it is still possible that nearly all the signal in the Kamiokande detector is due to ν_μ or, as in the scenario we consider, ν_τ, resulting from oscillations of the original ν_e.

It is interesting to note that the total detected rates in chlorine and gallium are both very close to twice that expected in the SSM for ^{7}Be neutrinos. To obtain this result we need an oscillation solution in which the low-energy pp and high-energy ^{8}B neutrinos are more suppressed than those from ^{7}Be. This can occur within the grand-unified theory (GUT) seesaw model when the large mass in the seesaw formula is close to the GUT scale. Then high-energy neutrinos are suppressed by ν_e-ν_τ oscillations but the low-energy neutrinos could be suppressed by the ν_e-ν_μ oscillations [13].

It should be emphasized that we have no reason to expect the deviations from the SSM considered here. The main purpose of this study is to point out how little we directly know from published solar neutrino experiments and how much

can be learned from SNO, BOREXINO, and other future experiments. The spirit of this discussion is similar to the demonstration in [12] that the existing experiments cannot, if neutrino oscillations occur, rule out a CNO energy generation scenario.

This paper is organized as follows. In Sec. II we discuss the range of possible beryllium neutrino fluxes assuming MSW transitions are taking place inside the Sun. The necessary conditions are formulated that would allow for the beryllium neutrino flux to take on its maximum allowed by the luminosity constraint value. The realization of these conditions in a scenario where three neutrinos take part in MSW transitions inside the Sun is described in Sec. III. The allowed parameter regions are found and the implications for neutrino masses are discussed. In Sec. IV we describe a three-neutrino MSW solution which assumes a 5% higher central temperature in the Sun than in the SSM. The beryllium neutrino flux in this solution turns out to dominate the event rates in both gallium and chlorine experiments. In Sec. V the expected event rates in the future detectors SuperKamiokande, SNO, BOREXINO, ICARUS, HELLAZ, and HERON are calculated. We also discuss some of the distinctive features of the signals in the future solar neutrino experiments the nonobservation of which will rule out the maximum ^{7}Be neutrino flux solution.

II. BERYLLIUM NEUTRINO FLUX

In this section we present in a simplified form the values of the fluxes from each of the major neutrino sources (pp, ^{7}Be, and ^{8}B) allowed by the present experimental data subject to the luminosity constraint and assuming MSW oscillations as a solution of the solar neutrino problem.

The luminosity constraint follows from energy conservation assuming the amount of energy emitted by the Sun is matched by the amount of energy produced in the nuclear reactions. It can be written as a linear relation between the neutrino fluxes from each neutrino source (pp, ^{7}Be, ^{8}B, etc.) [8]. Assuming essentially constant solar luminosity, the present value of which has been measured with a better than 1% accuracy, any solar model has to satisfy this constraint. As explained in [8] the luminosity constraint imposes upper limits on all neutrino fluxes. When the beryllium neutrino flux reaches its maximum value [$\Phi(^7\mathrm{Be}) = 3.33\times 10^{10}$ $\mathrm{cm}^{-1}\mathrm{s}^{-1}$], the pp neutrino flux is reduced by a factor of approximately 0.565 [assuming the same $p+e^-+p$ (pep)/pp flux ratio as in the SSM] and all the other neutrino fluxes should be zero. However, in order to explain the Kamiokande result, one has to account for a boron neutrino flux roughly between 0.3 and 3 times its standard solar model value [9]. As the boron neutrino contribution to the solar luminosity is very small this does not significantly change the upper limit on the beryllium neutrino flux.

In a simplified version, suitable for the discussion of the general ideas here, the luminosity constraint can be written as

$$f_{pp} = 1.10 - 0.083 f_{\mathrm{Be}}, \tag{1a}$$

$$f_{pp} \geqslant 0.087 f_{\mathrm{Be}}. \tag{1b}$$

The quantities f_α, where $\alpha = pp$, ^{7}Be, pep, ^{8}B, etc., are the ratios of the true fluxes to the ones predicted in the SSM: $\Phi(\alpha)/\Phi(\alpha)_{\mathrm{SSM}}$. The numerical coefficient in Eq. (1b) is equal to the ratio $[\Phi(^7\mathrm{Be})/\Phi(pp)]_{\mathrm{SSM}}$ of the ^{7}Be to pp neutrino flux in the SSM and follows from the fact that one pp reaction is needed to produce a ^{7}Be nucleus. It has been assumed in Eqs. (1) that $f_{\mathrm{CNO}} = 0.0$ and $f_{\mathrm{pep}} = f_{pp}$, i.e., that the ratio between pep and pp neutrino fluxes is the same as in the standard solar model.[1] As mentioned in the previous paragraph, from Eqs. (1) it follows that the maximum ^{7}Be neutrino flux is about 6.5 times the SSM ^{7}Be flux.

In order to find the fluxes and average survival probabilities, for which the scenario we consider here can provide a good fit to the data, we write the event rates in the three detectors (gallium, chlorine, and neutrino-electron scattering) as

$$Q_{\mathrm{Ga}} = f_{\mathrm{B}} P_{\mathrm{B}} Q_{\mathrm{Ga}}^{\mathrm{B}} + f_{\mathrm{Be}} P_{\mathrm{Be}} Q_{\mathrm{Ga}}^{\mathrm{Be}} + f_{pp} P_{pp} Q_{\mathrm{Ga}}^{pp}, \tag{2a}$$

$$Q_{\mathrm{Cl}} = f_{\mathrm{B}} P_{\mathrm{B}} Q_{\mathrm{Cl}}^{\mathrm{B}} + f_{\mathrm{Be}} P_{\mathrm{Be}} Q_{\mathrm{Cl}}^{\mathrm{Be}}, \tag{2b}$$

$$R_{\nu e} = f_{\mathrm{B}}(0.855 P_{\mathrm{B}} + 0.145). \tag{2c}$$

The quantities on the left-hand side of the first two equations are the event rates in the gallium and chlorine detectors, $R_{\nu e}$ is the ratio (measured ^{8}B flux)/(SSM ^{8}B flux). P_α is the average survival probability for neutrinos from source α and Q_i^α is the SSM contribution of source α in the ith radiochemical detector ($i = \mathrm{Ga}, \mathrm{Cl}$). Here we have neglected the ''minor'' solar neutrino sources, namely, the CNO and pep neutrinos. We have also assumed that the suppression factors P_{B} are the same for all three experiments and the factors P_{Be} are the same for chlorine and gallium. In reality these factors are different from experiment to experiment because the experiments do not cover the same energy range and also because the detector cross sections are slightly different functions of energy. These simplifications are made in this section, but not in Secs. III, IV, and V, in order to make more clear the general idea of the proposed scenario.

Equation (2c) is based on the fact that the Kamiokande detector is sensitive to ν_μ and ν_τ, as well as ν_e, with the cross section for ν_μ and ν_τ down by a factor of about 0.15. For $R_{\nu e} = 0.44$, as indicated by the Kamiokande result, when f_{B} is varied from 0.3 to about 3, the required value of P_{B} goes from one to zero. When f_{B} is close to its maximum allowed value nearly all the neutrinos observed by Kamiokande are ν_μ or ν_τ.

When we turn to the ^{37}Cl detector only the ν_e are effective. As a result, as P_{B} approaches zero, there is no ^{8}B neutrino signal and, neglecting ^{13}N and ^{15}O neutrinos, the detected rate must be almost entirely due to ^{7}Be neutrinos. This requires a ^{7}Be rate about twice the SSM value which in turn means that nearly all the signal in the gallium detector is due to ^{7}Be neutrinos.

[1] Note that $f_{pp} > 1$ for $f_{\mathrm{Be}} = 1$. This reflects the fact that, since for simplicity we have set the CNO neutrino flux has to zero, some of the other fluxes have to be larger than in the SSM in order to compensate for the approximately 2% of the luminosity that the CNO neutrinos account for in the SSM.

TABLE I. Fluxes and survival probabilities depending on the assumed boron neutrino flux (first column) which satisfy the constraints from the existing data (columns 2–5) which are then combined with the luminosity constraint and the specific energy dependence of the survival probability for nonadiabatic MSW transitions to get the last three columns.

f_B	P_B	$f_B P_B$	$f_{Be} P_{Be}$	$f_{pp} P_{pp}$	f_{Be}	P_{Be}	P_{pp}
1.0	0.34	0.34	0.0085	0.98	0.0089	0.96	0.89
1.5	0.17	0.26	0.51	0.72	0.58	0.88	0.69
2.0	0.088	0.17	1.02	0.47	1.31	0.77	0.48
2.5	0.036	0.091	1.52	0.22	2.48	0.61	0.24
2.9	0.008	0.023	1.92	0.017	6.46	0.30	0.031

Given the experimental results[2] $Q_{Ga} = 74 \pm 8$ SNU (combined GALLEX + SAGE result), $Q_{Cl} = 2.55 \pm 0.25$ SNU, and $R_{\nu e} = 0.44 \pm 0.06$, and the contributions of the individual sources to each experiment according to the SSM [1], which includes helium and heavy element diffusion, we can solve Eqs. (2) for the products $f_\alpha P_\alpha$, assuming different boron neutrino fluxes. The first five columns of Table I summarize the results of this simple calculation using the central values of the experiments.

For the last three rows of Table I the value of $f_{Be} P_{Be}$ is greater than unity, which means that half or more of the detected flux in the chlorine and gallium detectors is due to ^{7}Be neutrinos. The last row corresponds to the extreme case that nearly all of these fluxes is due to ^{7}Be. In order to get the large suppression needed for the pp neutrinos for such a solution we require $P_{pp} < P_{Be}$. This can be achieved by arranging for a nonadiabatic MSW oscillation to suppress these fluxes.

The survival probability in the nonadiabatic regime is given to a good approximation by a simple function of energy, namely, $P = \exp(-C/E_\nu)$, where $C = \pi \Delta m^2 \sin^2 2\theta / 4 \cos 2\theta N_e'$, N_e' is the logarithmic derivative of the electron density at the resonance, and E_ν is the neutrino energy. Thus it is not possible to have very small P_{pp}, e.g., $P_{pp} = 0.1$ and $P_{Be} \simeq 1$. Using the nonadiabatic survival probability for ^{7}Be (0.862 MeV) and pp neutrinos (assuming average pp neutrino energy $E_{pp} = 0.3$ MeV) to find the relation $P_{pp} = P_{Be}^{2.87}$, one can then use Eq. (1a) together with the values of $f_{pp} P_{pp}$ and $f_{Be} P_{Be}$ to determine the values of f_{Be}, P_{Be}, and P_{pp} given in the last three columns of Table I.

The last row of Table I illustrates the case in which the initial beryllium neutrino flux is close to the maximum allowed by the luminosity constraint ($f_{Be} = 6.46$). In the next section we explore solutions of this type in the three-neutrino oscillation scenario. A similar large beryllium neutrino flux can be fitted with two-neutrino oscillations [8], but in that case the pp flux is not suppressed and the ^{7}Be neutrino contribution does not dominate the signal in the gallium detector.

III. THREE-NEUTRINO OSCILLATION SCENARIO

Here we discuss the three-neutrino survival probabilities and the allowed regions that we obtain for the neutrino mixing angles and mass-squared differences for the particular example in which the beryllium neutrino flux has its maximum allowed by the luminosity constraint value.

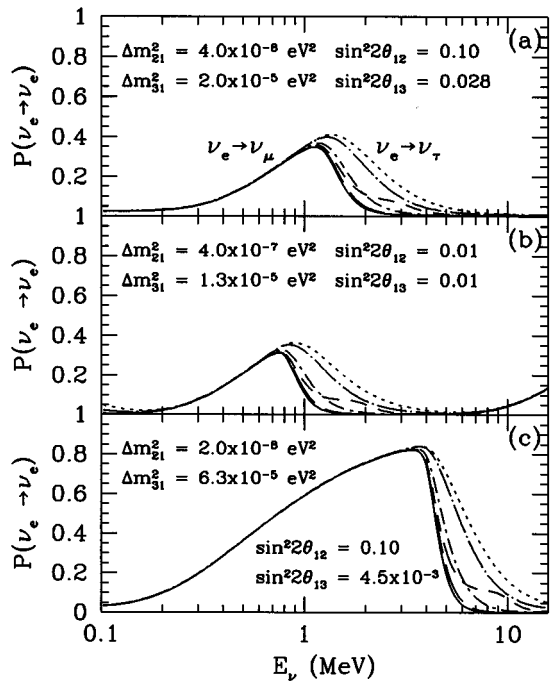

FIG. 1. Neutrino survival probabilities averaged over the relevant neutrino production regions (dotted line pp, short-dash-dotted line ^{7}Be, solid line ^{8}B, short-dashed line ^{13}N, long-dashed line ^{15}O, long-dash-dotted line pep) are shown as a function of energy. The neutrino mass-squared differences and mixing angles are indicated in each panel. The type of the dominant transition ($\nu_e \rightarrow \nu_\mu$ or $\nu_e \rightarrow \nu_\tau$) is indicated on both sides of the peak in the first panel.

In the general case of three-neutrino oscillations [14] the electron neutrino survival probability is a complicated function of the mixing angles θ_{12} and θ_{13} of the mass-squared differences Δm^2_{21} and Δm^2_{31} and of the density distribution along the neutrino path. The existing analytic expressions [15] for $P(\nu_e \rightarrow \nu_e)$ in this case are far from transparent and not easy to implement in a numerical calculation. However, as shown in [16], when certain conditions on the neutrino mass and mixing parameters are satisfied, the three-neutrino survival probability can be written down as a product of two-neutrino survival probabilities plus a residual term which is suppressed by a coefficient dependent on the mixing angles. In the limit of small mixing angles and sufficiently large separation between the positions (in space) of the resonant transition regions the residual term is vanishingly small. In our calculations we have neglected this residual term. In most of the interesting situations discussed here we have verified that it is indeed small and does not contribute more than a few percent to the overall electron-neutrino survival probability, which is sufficiently accurate for our purposes.

Using the product of the two two-neutrino survival probabilities, for each of which we apply the analytical description from [17], we have been able to study numerically a large number of interesting cases. Three characteristic sets of neutrino survival probability curves are displayed in Fig. 1. The survival probabilities have been averaged over the rel-

[2]We have combined quadratically the statistical and systematic errors for each experiment.

TABLE II. Event rates in the operating experiments (three neutrino oscillations, maximum ^{7}Be neutrino flux). The values in the table are in SNU for chlorine and gallium and the ratio (observed ^{8}B flux)/(SSM ^{8}B flux) is given for Kamiokande. The neutrino mass and mixing angles are given in the text and correspond to the black dot in Fig. 2(d). The last line in the table gives the ratios of the assumed neutrino fluxes to the ones in the SSM [1].

Experiment	pp	^{8}B	^{7}Be(0.862)	^{7}Be(0.384)	^{13}N	^{15}O	pep	Total
Gallium	2.6	0.30	70.2	0.70	0.0	0.0	0.65	74.5
Chlorine	-	0.14	2.38	-	0.0	0.0	0.05	2.57
Kamioka	-	0.44	-	-	-	-	-	0.44
f_α	0.56	2.9	6.46	6.46	0.0	0.0	0.56	

evant production region (as calculated in the SSM) of each neutrino source and are indicated with different lines. In all three figures the transitions in the energy region to the left of the peak (lower than the energy at the maximum) are predominantly $\nu_e \rightarrow \nu_\mu$ and those to the right of the peak (higher than the energy at the maximum) are predominantly $\nu_e \rightarrow \nu_\tau$. The position of the peak, its height, and width are determined by all four parameters indicated in each panel. For the maximum ^{7}Be neutrino flux solution the width of the peak is not very important because the CNO neutrino flux is negligible in this case. Changes in θ_{13} do not affect strongly the peak, but are very important for the suppression of the high-energy boron neutrino flux; e.g., in Fig. 1(b), the high-energy part of the boron neutrino flux is less suppressed than in Fig. 1(a). The curves in Figs. 1(a) and 1(b) at energies below about 0.8 MeV coincide except for energies $E_\nu < 0.2$ MeV, which is below the threshold (0.233 MeV) of the gallium experiments. This is explained by the fact that the ascending parts of the curves represent the nonadiabatic branches of the two-neutrino survival probabilities. The latter depend mainly on the product $\Delta m^2 \sin^2 2\theta$ which is the same in both panels. In Fig. 1(c) the flux of the low-energy, pp and ^{7}Be, neutrinos are more strongly suppressed than the flux of the intermediate-energy (CNO) neutrinos. Most of the ^{8}B neutrino flux, essentially all above 6 MeV, is strongly suppressed.

Without a solar model that could provide the neutrino fluxes envisaged in the scenario under discussion one might think that the survival probabilities so described are very uncertain. However, any solar model will have to have approximately the same density distribution, exponential to a high degree of accuracy, if it describes a star in hydrostatic equilibrium. Note also that helioseismology provides independent information about the density distribution inside a large part of the solar interior. Although the neutrino production regions cannot be expected to be the same as in the standard solar model, their exact shapes are not so important as it might seem. Note that in the energy region of the pp, ^{7}Be, and ^{8}B neutrinos the survival probability curves essentially coincide (see Fig. 1). The difference is largest in the region of the intermediate-energy neutrinos which are relatively unimportant in the scenario discussed here.

Using the so-described analytical approximation of the three-neutrino ν_e survival probability we have performed an analysis of the solar neutrino data from the four operating experiments in a way similar to the standard analysis for the two-neutrino MSW solution. Our goal is to find allowed regions in parameter space in which it is possible to fit all the experimental results with a maximum beryllium neutrino flux. First we choose the pp, pep, ^{7}Be, and CNO neutrino fluxes so that they correspond to the maximum beryllium neutrino flux allowed by the luminosity constraint assuming the SSM pep/pp flux ratio. The requirement of maximal ^{7}Be neutrino flux automatically sets the CNO fluxes to zero. The values of all flux ratios $[\Phi(\alpha)/\Phi(\alpha)_{\rm SSM}]$ are given in the last line of Table II. We then vary the boron neutrino flux within 0.44 to about 3 times its SSM value, i.e., within the limits set by the Kamiokande result. In addition to the ^{8}B flux we vary the parameters Δm^2_{21}, Δm^2_{31}, $\sin^2 2\theta_{12}$, and $\sin^2 2\theta_{13}$ and compute the χ^2 taking into account detection cross-section uncertainties and experimental errors. Once we

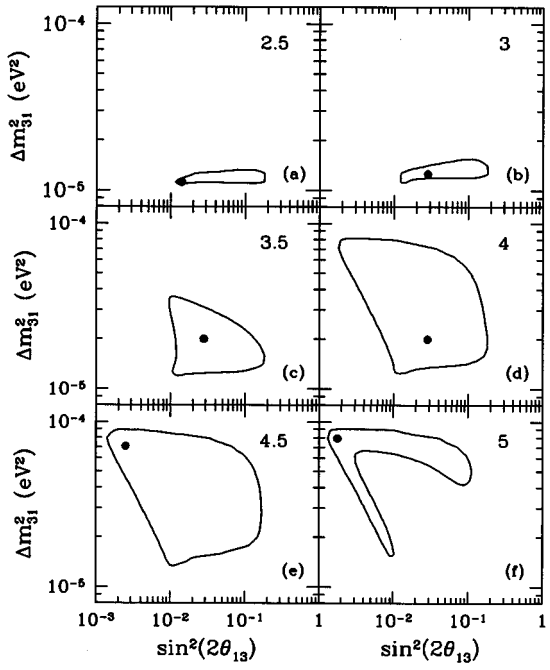

FIG. 2. Allowed regions at 95% C.L. in the mass-mixing plane (Δm^2_{31}-$\sin^2 2\theta_{13}$). The other two-neutrino oscillation parameters are fixed: For each of the six panels $\sin^2 2\theta_{12} = 0.1$ and the values of Δm^2_{21} are given in units of 10^{-8} eV^2 in the upper right corner of each panel. The point in the mass-mixing plane where the χ^2 is minimum is indicated with a black dot. The boron neutrino flux is equal to $2.9\Phi(^8{\rm B})_{\rm SSM}$, the pp neutrino flux is 56% of the SSM value, and the beryllium neutrino flux is equal to 99.9% of the maximum allowed by the luminosity constraint value (3.33×10^{10} cm^{-2} s^{-1}).

TABLE III. Event rates in the operating experiments (three neutrino oscillations, $T_c = 1.05 T_c^{SSM}$). The values in the table are in SNU for chlorine and gallium and the ratio (observed ^{8}B flux)/(SSM ^{8}B flux) is given for Kamiokande. The neutrino mass and mixing angles are given in the text. The last line in the table gives the ratios of the assumed neutrino fluxes to the ones in the SSM [1].

Experiment	pp	^{8}B	^{7}Be(0.862)	^{7}Be(0.384)	^{13}N	^{15}O	pep	Total
Gallium	13.7	1.00	32.4	0.55	5.82	15.0	1.83	70.3
Chlorine	-	0.18	1.10	-	0.19	1.10	0.13	2.70
Kamioka	-	0.48	-	-	-	-	-	0.48
f_α	0.90	3.22	1.63	1.63	3.29	3.75	0.90	

have found a value of the boron neutrino flux [$\Phi(^8\mathrm{B}) = 2.9$] for which χ^2 is sufficiently small (typically $\chi^2 < 0.7$), we then keep the ^{8}B flux, Δm^2_{21}, and $\sin^2 2\theta_{12}$ fixed and repeat the calculation varying only Δm^2_{31} and $\sin^2 2\theta_{13}$, the two parameters corresponding to the high-energy resonance. We repeat the same procedure for several pairs of Δm^2_{21} and $\sin^2 2\theta_{12}$ close to the ones for which a sufficiently small χ^2 has been found. The resulting 95% C.L.-allowed regions (corresponding to $\chi^2 = \chi^2_{\min} + 5.99$ for two degrees of freedom) in the two parameters, Δm^2_{31} and $\sin^2 2\theta_{13}$, are shown in Fig. 2. In each of the six panel $\sin^2 2\theta_{12} = 0.1$ and the values of Δm^2_{12} are indicated in the upper right corner. As noted before the results depend primarily on the product $\Delta m^2_{21} \sin^2 2\theta_{12}$. Therefore quite similar plots as those shown in Fig. 2 can be obtained for different Δm^2_{21} and $\sin^2 2\theta_{12}$ the product of which is the same as in the six panels of Fig. 2. The black dots indicate the position of the best-fit point in each case. The survival probability for the best fit solution in Fig. 2(d) is the one displayed in Fig. 1(a); the corresponding event rates expected in each of the four operating experiments are given in Table II for the best-fit solution. The resulting event rates in the four experiments in this case correspond to mainly beryllium neutrinos contributing in all radiochemical experiments and Kamiokande detecting only ν_τ but virtually no ν_e from the Sun.

The solutions shown correspond to the extreme possibility of a maximum beryllium neutrino flux. Somewhat similar solutions could be found for less extreme cases such as those illustrated by the third and fourth rows of Table I. As the values of f_B (and f_{Be}) go down the value of Δm^2_{21} is decreased and that of Δm^2_{31} is increased for given values of θ_{12} and θ_{13}. This yields an increase in the peak of the survival probability curve which corresponds approximately to P_{Be}.

The values of Δm^2_{31} correspond to a ν_τ mass of the order a few times 10^{-3}eV in qualitative agreement with the seesaw formula with large mass near the GUT scale. The ν_μ mass can then be chosen a factor of 30 or so lower in general agreement with the assumption of a mass hierarchy, although many detailed GUT models give a significantly larger ratio.

IV. HIGH T_c SCENARIO

The nuclear reactions in which solar neutrinos are produced take place in a hot plasma and the neutrino fluxes are functions of the temperature. The effective temperature dependences of the neutrino fluxes in the standard solar model [1] have recently been estimated [18]:

$$\phi(pp) \propto [1 - 0.08 (T_c / T_{c,\mathrm{SSM}})^{-11}], \tag{3a}$$

$$\phi(\mathrm{pep}) \propto (T_c / T_{c,\mathrm{SSM}})^{-2.4}, \tag{3b}$$

$$\phi(^8\mathrm{B}) \propto (T_c / T_{c,\mathrm{SSM}})^{24}, \tag{3c}$$

$$\phi(^7\mathrm{Be}) \propto (T_c / T_{c,\mathrm{SSM}})^{10}, \tag{3d}$$

$$\phi(^{13}\mathrm{N}) \propto (T_c / T_{c,\mathrm{SSM}})^{24.4}, \tag{3e}$$

$$\phi(^{15}\mathrm{O}) \propto (T_c / T_{c,\mathrm{SSM}})^{27.1}. \tag{3f}$$

From Eqs. (3) it is clear that in solar models with higher central temperature (and no radically new physics) the pp neutrino flux will be reduced, whereas the ^{7}Be and ^{8}B neutrino fluxes will be enhanced. As discussed in the previous section, these changes are in the direction of the ones needed in the scenario where the ^{7}Be neutrinos are the major component of the signal in the radiochemical experiments. Because of the strong temperature dependence of most of the fluxes, it turns out that it is possible to find a solution with ^{7}Be neutrino dominance for[3] $(T - T_c)/T_c = 0.05$. The solution that we have found is described in Table III. The ''best-fit'' ($\chi^2_{\min} = 0.7$) neutrino oscillation parameters are $\Delta m^2_{21} = 2 \times 10^{-8}$ eV^2, $\Delta m^2_{31} = 6.3 \times 10^{-5}$ eV^2, $\sin^2 2\theta_{12} = 0.1$, and $\sin^2 2\theta_{13} = 4.5 \times 10^{-3}$. The survival probability averaged over the different neutrino production regions in the Sun is given in Fig. 1(c). The major component of the signal in the radiochemical detectors comes from ^{7}Be neutrinos. The pp neutrino event rate in the gallium detectors is about 2.5 times lower than the one due to beryllium neutrinos. The allowed region in the Δm^2_{31}-$\sin^2 2\theta_{13}$ plane for fixed Δm^2_{21} and $\sin^2 2\theta_{12}$ is given in Fig. 3 where the black dot indicates the ''best-fit'' solution.

We want to emphasize that we do not introduce any particular mechanism to change the central temperature of the Sun. It should be noted that the temperature dependence given in Eqs. (3) has been derived from a set of models in which the temperature varied by less than 2% and our extension to a change of 5% is not necessarily justified. Furthermore, there exists helioseismological evidence against such a large central temperature [19]; however, our goal has been to see what can be learned from neutrino data alone.

[3] In order to satisfy the luminosity constraint we have reduced the pp neutrino flux by 2.5% from the value prescribed by Eq. (3a). For all other fluxes we have used values given by Eqs. (3).

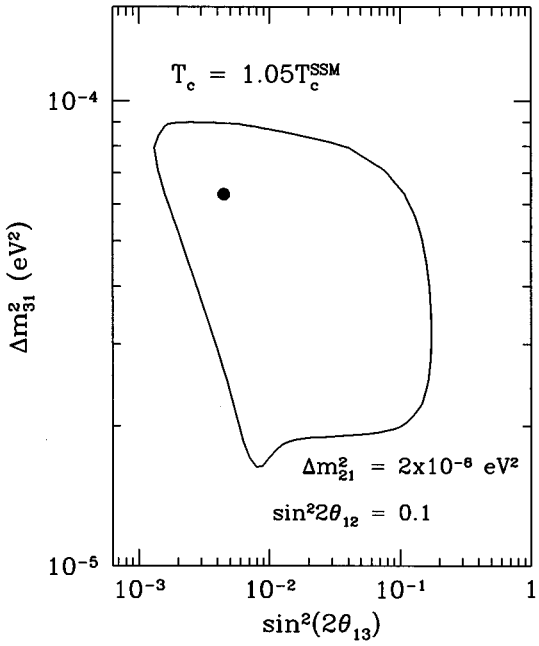

FIG. 3. Allowed region at 95% C.L. in the mass-mixing plane (Δm^2_{31}-$\sin^2 2\theta_{13}$) corresponding to neutrino fluxes in a solar model with $T_c = 1.05 T_{c,\mathrm{SSM}}$. The neutrino oscillation parameters Δm^2_{21} and $\sin^2 2\theta_{12}$ are fixed and their values are indicated in the panel. The black dot corresponds to the point in the mass-mixing plane where the χ^2 is minimum. The ratio of the neutrino fluxes to those in the SSM are given in the last line of Table III.

V. FUTURE DETECTORS

The scenarios we consider here have important implications for the SNO [20] detector. In the set of possibilities shown in Table I, $f_B P_B$ gives the ratio of the charged current (CC) event rate to the same rate in the SSM without oscillations. This varies from about one-third (the value for the standard MSW solution) to close to zero in the extreme case. SNO can distinguish the CC events on deuterium ($\nu_e + d \rightarrow p + p + e^-$) from the neutrino electron scattering because the latter are strongly forward peaked, whereas the former are weakly backward peaked. Thus for the first time the rate of ν_e arriving from ^{8}B will be measured. The smaller the ratio of charged current events to those from (νe) scattering, the larger the flux of ν_τ or ν_μ compared to ν_e must be. In some of the solutions the spectrum of the charged current events may be distorted; for example, for the case shown in Fig. 1(b) the spectrum is suppressed at low energies and rises at high energies relative to the normal ^{8}B spectrum.

SNO will also measure the rate of neutral current disintegration of deuterium (NC) ($\nu + d \rightarrow p + n + \nu$) which is directly proportional to f_B and is independent of oscillations between active neutrinos. For the set of possibilities shown in Table I as the charged current event rate decreases the neutral current one increases, yielding the possibility of a very large neutral current to charged current ratio.

SuperKamiokande [21] measures only neutrino-electron scattering from ^{8}B neutrinos, the overall rate of which was already determined by the earlier Kamiokande experiment. This experiment is sensitive to significant distortions in the spectrum of detected neutrinos. In the extreme case we consider in which nearly all the neutrinos detected are ν_μ and ν_τ there is very little or no distortion at all. The day-night effect which could occur because of regeneration of ν_e in the Earth is not expected for the values of Δm^2 in our solutions.

Future detectors such as BOREXINO [22], ICARUS [23], HERON [24], and HELLAZ [25] might become operational in about 5–10 years. BOREXINO will be the first detector to directly measure the beryllium neutrino flux. According to the standard two-neutrino MSW solution based on the SSM, this detector is unlikely to measure any ^{7}Be flux above background whereas in the solution discussed in Sec. III the detected flux could be more than a factor of two greater than in the SSM. HERON and HELLAZ could be the first detectors to directly measure the pp neutrino flux. It is generally believed that the pp neutrinos are little affected by MSW oscillations but in the solutions considered here the arriving flux of pp neutrinos may be severely suppressed and the spectrum distorted.

Table IV summarizes our predictions for the event rates in future detectors in two scenarios with beryllium neutrino flux higher than in the SSM; these are compared to the predictions of the standard two-neutrino MSW solutions. The first line corresponds to the solution where the ^{7}Be neutrino flux is 6.46 times higher than in the SSM and almost equal to the maximum allowed by the luminosity constraint. The second line corresponds to the solution for neutrino fluxes from a hypothetical solar model with a central temperature higher by 5% than the one in the SSM. The normalized CC/NC double ratio $[(\mathrm{CC/CC_{SSM}})/(\mathrm{NC/NC_{SSM}})]$ in SNO can be obtained from the column corresponding to the SNO(CC) event rate by dividing by f_B (2.9 for the first line and 3.22 for the

TABLE IV. Ranges of event rates in the future experiments for (a) three-neutrino oscillations, maximum ^{7}Be neutrino flux; (b) $T_c = 1.05 T_{c,\mathrm{SSM}}$; (c) small mixing-angle two-neutrino MSW solution (SMA); and (d) large mixing-angle two-neutrino MSW solution (LMA). Each entry in the table represents the range of the ratio of the predicted event rate in the corresponding scenario to the event rate assuming SSM fluxes and no oscillations. The central value of the ratio corresponds to ''best-fit'' neutrino oscillation parameters in the relevant case. The neutrino mass and mixing angles are given in the text for the first two solutions and in [8] for the SMA and LMA solutions.

Scenario	SuperK	SNO(CC)	BOREXINO	ICARUS	HELLAZ/HERON
Maximum ^{7}Be	$0.45^{+0.12}_{-0.01}$	$0.019^{+0.10}_{-0.012}$	$2.88^{+0.06}_{-0.39}$	$0.019^{+0.10}_{-0.012}$	$0.20^{+0.0}_{-0.0}$
High T_c	$0.51^{+0.24}_{-0.02}$	$0.012^{+0.15}_{-0.005}$	$1.04^{+0.0}_{-0.20}$	$0.010^{+0.14}_{-0.002}$	$0.41^{+0.0}_{-0.01}$
SMA (2ν)	$0.41^{+0.19}_{-0.13}$	$0.32^{+0.23}_{-0.16}$	$0.22^{+0.50}_{-0.01}$	$0.34^{+0.23}_{-0.18}$	$0.96^{+0.04}_{-0.31}$
LMA (2ν)	$0.34^{+0.09}_{-0.06}$	$0.22^{+0.23}_{-0.06}$	$0.59^{+0.13}_{-0.14}$	$0.22^{+0.11}_{-0.06}$	$0.73^{+0.06}_{-0.08}$

second line). The results for BOREXINO include only the neutrino-electron scattering events originating from ^{7}Be neutrinos and include the contribution from $(\nu_\mu e)$ and/or $(\nu_\tau e)$ scattering. The high event rate in BOREXINO in the maximum beryllium neutrino scenario could be a clear signal of oscillations because it requires a contribution from ν_μ or ν_τ neutrinos in order to be consistent with the measured ν_e rates in gallium and chlorine.

VI. CONCLUSIONS

The ultimate goal of solar neutrino experiments is to learn about the nuclear reactions in the Sun and about possible neutrino oscillations. Given the limited present data the standard approach has been to use a standard model for the Sun and deduce neutrino oscillation parameters. These yield the result that practically no ν_e from ^{7}Be have been detected.

Here we relax the constraints on the fluxes from the SSM, keeping intact only the luminosity constraint, and demonstrate that the present data are consistent with the possibility of nearly all the ν_e detected in radiochemical detectors being from ^{7}Be and that nearly all the signal in the Kamiokande detector in this case could arise from ν_μ or ν_τ scattering from electrons. The neutrino oscillation parameters required are qualitatively consistent with neutrino masses and mixing suggested by some grand unified theories.

The major goal of this exercise is to emphasize how little is directly known about the solar neutrino flux arriving on the Earth and the importance of future experiments, particularly SNO, BOREXINO, HELLAZ, and HERON, which will be the first experiments to directly measure the ν_e flux from ^{8}B decay and the $^7\mathrm{Be}+p$ and pp reactions.

ACKNOWLEDGMENTS

The work of L.W. was partially supported by the U.S. Department of Energy Contract No. DE-FG 02-91 ER40682. The work of P.K. was partially supported by NSF Grant No. PHY-9513835. We are thankful to J. Bahcall and K. S. Babu for useful discussions. P.K. acknowledges support by the Theory Group at Fermilab for their summer visitor program during which part of this work was completed.

[1] J. Bahcall and M. Pinsonneault, Rev. Mod. Phys. **67**, 1 (1995); for a detailed description of the physics involved in solar modeling see J. N. Bahcall, *Neutrino Astrophysics* (Cambridge University Press, Cambridge, England, 1989).

[2] KAMIOKANDE Collaboration, Y. Suzuki, in *Neutrino 94*, Proceedings of the 16th International Conference on Neutrino Physics and Astrophysics, Eilat, Israel, edited by A. Dar *et al.* [Nucl. Phys. B (Proc. Suppl.) **38**, 54 (1995)]; K. S. Hirata *et al.*, Phys. Rev. D **44**, 2241 (1991).

[3] B. T. Cleveland *et al.*, in *Neutrino 94* [2], p. 47; R. Davis, Prog. Part. Nucl. Phys. **32**, 13 (1994).

[4] GALLEX Collaboration, P. Anselmann *et al.*, Phys. Lett. B **327**, 377 (1994); **342**, 440 (1995); **357**, 237 (1995).

[5] SAGE Collaboration, G. Nico *et al.*, in *Proceedings of the XXVII International Conference on High Energy Physics*, Glasgow, Scotland, 1994, edited by P. J. Bussey and I. G. Knowles (Institute of Physics, Bristol, 1995), p. 965; J. N. Abdurashitov *et al.*, Phys. Lett. B **328**, 234 (1994).

[6] J. N. Bahcall and H. Bethe, Phys. Rev. D **47**, 1298 (1993); P. Rosen and W. Kwong, Phys. Rev. Lett. **73**, 369 (1994); J. N. Bahcall, Phys. Lett. B **338**, 276 (1994); S. Parke, Phys. Rev. Lett. **74**, 839 (1995); N. Hata and P. Langacker, Phys. Rev. D **52**, 420 (1995).

[7] J.N. Bahcall, presented at the symposium on The Inconstant Sun, Naples, Italy, 1996, edited by G. Cauzzi and C. Marmolino, Memorie della Societa (to be published).

[8] J. N. Bahcall and P. I. Krastev, Phys. Rev. D **53**, 4211 (1996).

[9] P. I. Krastev and S. T. Petcov, Phys. Rev. D **53**, 1665 (1996).

[10] P. I. Krastev and A. Yu. Smirnov, Phys. Lett. B **338**, 282 (1994).

[11] N. Hata and P. Langacker, Phys. Rev. D **50**, 632 (1994).

[12] J. N. Bahcall , M. Fukugita, and P. I. Krastev, Phys. Lett. B **374**, 1 (1996).

[13] L. Wolfenstein, Phys. Rev. D **45**, R4365 (1992).

[14] T. K. Kuo and J. Pantaleone, Phys. Rev. D **35**, 3432 (1987); S. Toshev, Phys. Lett. B **185**, 177 (1987); **192**, 478(E) (1987); S. T. Petcov and S. Toshev, *ibid.* **187**, 120 (1987); S. T. Petcov, *ibid.* **214**, 259 (1988).

[15] E. Torrente Lujan, Phys. Rev. D **53**, 4030 (1996).

[16] A. Yu. Smirnov, Sov. J. Nucl. Phys. **46**, 672 (1987) [Yad. Fiz. **46**, 1152 (1987)].

[17] P. I. Krastev and S. T. Petcov, Phys. Lett. B **207**, 64 (1988).

[18] J. N. Bahcall and A. Ulmer, Phys. Rev. D **53**, 4202 (1996).

[19] J. N. Bahcall and M. Pinsonneault, Phys. Rev. Lett. **78**, 171 (1997).

[20] H. H. Chen, Phys. Rev. Lett. **55**, 1534 (1985); G. Ewan *et al.*, Sudbury Neutrino Observatory Proposal No. SNO-87-12, 1987 (unpublished); A. B. McDonald, in *Proceedings of the Ninth Lake Louise Winter Institute*, edited by A. Astbury *et al.* (World Scientific, Singapore, 1994), p. 1.

[21] M. Takita, in *Frontiers of Neutrino Astrophysics*, edited by Y. Suzuki and K. Nakamura (Universal Academy Press, Tokyo, 1993), p. 147; T. Kajita, ''Physics with the SuperKamiokande Detector,'' ICRR Report No. 185-89-2, 1989 (unpublished).

[22] C. Arpesella *et al.*, BOREXINO proposal, Vols. 1 and 2, edited by G. Bellini *et al.*, University of Milano, Milano, 1992 (unpublished); R. S. Raghavan, Science **267**, 45 (1995).

[23] A First 600 Ton ICARUS Detector Installed at the Gran Sasso Laboratory, addendum to Proposal No. LNGS-94/99 I&II, Report No. LNGS-95/10, 1995 (unpublished); J. N. Bahcall, M. Baldo-Ceolin, D. Cline, and C. Rubbia, Phys. Lett. B **178**, 324 (1986).

[24] S. R. Bandler *et al.*, J. Low Temp. Phys. **93**, 785 (1993); R. E. Lanou, H. J. Maris, and G. M. Seidel, Phys. Rev. Lett. **58**, 2498 (1987).

[25] G. Laurenti *et al.*, in *Proceedings of the Fifth International Workshop on Neutrino Telescopes, Venice, Italy, 1993*, edited by M. Baldo Ceolin (Padua University, Padua, Italy, 1994).